Supplemental Material can be found at:
http://www.jbc.org/cgi/content/full/M607159200/DC1

THE JOURNAL OF BIOLOGICAL CHEMISTRY VOL. 282, NO. 16, pp. 12230–12239, April 20, 2007
© 2007 by The American Society for Biochemistry and Molecular Biology, Inc. Printed in the U.S.A.

The "Jaws" of the Tau-Microtubule Interaction*[S]

Received for publication, July 27, 2006, and in revised form, February 15, 2007 Published, JBC Papers in Press, February 15, 2007, DOI 10.1074/jbc.M607159200

Marco D. Mukrasch[‡], Martin von Bergen[§], Jacek Biernat[§], Daniela Fischer[‡], Christian Griesinger[‡], Eckhard Mandelkow[§], and Markus Zweckstetter[‡1]

From the [‡]Department for NMR-based Structural Biology, Max Planck Institute for Biophysical Chemistry, Am Fassberg 11, 37077 Göttingen and the [§]Max Planck Unit for Structural Molecular Biology, c/o DESY, Notkestrasse 85, 22607 Hamburg, Germany

Tau is the major microtubule-associated protein in neuronal axons. It aggregates into "neurofibrillary tangles" during the course of Alzheimer disease. Binding to microtubules and microtubule assembly requires the "repeat domain" in the C-terminal half of Tau, as well as the two regions flanking the repeats. Here we report the NMR characterization of a 198-residue Tau fragment composed of the four tandem repeats and the flanking domains and containing the full microtubule binding and assembly activity of Tau. NMR secondary chemical shifts and dipolar couplings detect the highest propensity for β-structure within the four-repeat region, whereas the flanking domains are largely random coil, with an increased rigidity in the proline-rich region. Chemical shift perturbation experiments identify two motifs in the upstream flanking domain, ^{225}KVAVVRT^{231} and ^{243}LQTA^{246}, and one downstream of the repeats, ^{370}KIETHKTFREN^{380}, which strongly contribute to the binding to the acidic outside of microtubules, as well as to the binding of other polyanions such as heparin. This is consistent with the "jaws" model of Tau-microtubule interactions and highlights the importance of the regions flanking the repeats for both microtubule binding and pathological Tau aggregation.

Tau, the major MAP[2] of neurons, is localized predominantly in axons. Tau stabilizes MTs and is necessary for neurite outgrowth (1, 2). Tau occurs in six main isoforms in the human brain (ranging between 352 and 441 amino acid residues), obtained by alternative splicing, and differs by having 3 or 4 semi-conserved repeats of ~31 residues in the MT assembly domain and 0–2 insertions in the N-terminal projection domain (Fig. 1) (3, 4). The repeat domain is important for promoting microtubule assembly, but it binds to microtubules only with low affinity. However, strong MT binding and efficient assembly is achieved when the repeat domain is combined with the flanking domains, whereas the flanking domains alone bind to microtubules but do not promote MT assembly. This leads to the proposition of the "jaws" model of Tau whereby the flanking regions are considered as targeting domains, responsible for positioning Tau on the MT surface, and the repeats are considered as catalytic domains for MT assembly (5, 6).

In Alzheimer disease, Tau aggregates into neurofibrillary tangles, which consist of "paired helical filaments" (PHFs) (7, 8). The repeat domain coincides with the core of PHFs (9–11) and promotes PHF assembly *in vitro* (12). For PHF aggregation, two hexapeptides at the beginning of the second and third repeats (^{275}VQIINK^{280} and ^{306}VQIVYK^{311}) are crucial (13, 14). The role of the repeat domain both in MT assembly and PHF aggregation illustrates a remarkable overlap between physiological and pathological functions of Tau. Both functions are regulated by phosphorylation, whereby the phosphorylation of the repeat domain (K*X*GS motifs) efficiently detaches Tau from microtubules and prevents PHF aggregation, whereas phosphorylation in the flanking domains has a modulating effect (15).

To gain a structural understanding of the MT binding and PHF aggregation activities, we performed a detailed NMR characterization of a 198-residue fragment (construct K32), containing the repeat domain and the two flanking domains. Tau is a natively unfolded protein so that x-ray crystallography cannot be applied, leaving NMR spectroscopy as almost the only method that allows detailed structure information. The results presented here provide a view of the jaws in Tau that are essential for efficient binding of Tau to microtubules.

EXPERIMENTAL PROCEDURES

Expression and Isotopic Labeling of Recombinant Tau Constructs—Human Tau constructs were expressed in the vector pNG2 (a derivative of pET-3a; Merck) in *Escherichia coli* strain BL21(DE3) as described (5) (see Fig. 1). K32 comprises residues (Met)Ser^{198}–Tyr^{394}, equivalent to the four repeats and the two flanking regions (198 residues). The expressed proteins were purified from bacterial extracts by making use of the heat stability of the protein and by FPLC SP-Sepharose chromatography (Amersham Biosciences). To label the Tau proteins with ^{15}N- and ^{13}C-stable isotopes, the *E. coli* culture expressing the K32 protein was grown on rich growth medium based on chemolithoautotrophic bacteria labeled with ^{13}C and ^{15}N isotopes (Silantes, Munich, Germany). Protein samples uniformly enriched in ^{15}N were prepared by growing *E. coli* bacteria in minimal medium containing 1g liter^{-1} of $^{15}NH_4Cl$.

* This work was supported by the Max Planck Society (to E. M. and C. G.), the European Union through Understanding Protein Misfolding and Aggregation by NMR (to M. Z.), the Fonds der Chemischen Industrie, the Boehringer Ingelheim Fonds (to M. D. M.), Deutsche Forschungsgemeinschaft Grant GK 782 (to C. G. and M. D. M.), and Deutsche Forschungsgemeinschaft Emmy Noether Fellowship ZW 71/1-5 (to M. Z.). The costs of publication of this article were defrayed in part by the payment of page charges. This article must therefore be hereby marked "*advertisement*" in accordance with 18 U.S.C. Section 1734 solely to indicate this fact.

[S] The on-line version of this article (available at http://www.jbc.org) contains supplemental Figs. S1–S5 and a table.

[1] To whom correspondence should be addressed. Tel.: 49-551-201-2220; Fax: 49-551-201-2202; E-mail: mzwecks@gwdg.de.

[2] The abbreviations used are: MAP, microtubule-associated protein; MT, microtubule; PHF, paired helical filament; NOE, nuclear Overhauser effect; DTT, dithiothreitol; MES, 4-morpholineethanesulfonic acid; Pipes, 1,4-piperazinediethanesulfonic acid; RDC, residual dipolar coupling; HSQC, heteronuclear single quantum coherence.

Downloaded from www.jbc.org at Max Planck Inst.Biophysikalische Chemie,Otto Hahn Bibl,Pf.2841,37018 Goettingen on March 23, 2009

The cell pellets were resuspended in boiling extraction buffer (50 mM MES, 500 mM NaCl, 1 mM $MgCl_2$, 1 mM EGTA, 5 mM DTT, pH 6.8) complemented with a protease inhibitor mixture. The cells were disrupted with a French pressure cell and subsequently boiled for 20 min. The soluble extract was isolated by centrifugation, and the supernatant was dialyzed against two changes of cation exchange chromatography buffer A (20 mM MES, 50 mM NaCl, 1 mM EGTA, 1 mM $MgCl_2$, 2 mM DTT, 0.1 mM phenylmethylsulfonyl fluoride, pH 6.8) and loaded on an FPLC SP-Sepharose column. The proteins were eluted by a linear gradient of cation exchange chromatography buffer B (20 mM MES, 1 M NaCl, 1 mM EGTA, 1 mM $MgCl_2$, 2 mM DTT, 0.1 mM phenylmethylsulfonyl fluoride, pH 6.8). In the second purification step, the K32 breakdown products were removed by applying the gel filtration column Superdex G-75 with PBS buffer (137 mM NaCl, 3 mM KCl, 10 mM Na_2HPO_4, 2 mM KH_2PO_4, pH 7.4, with 1 mM DTT). NMR samples contained 0.9 to 1.5 mM ^{15}N- or $^{15}N/^{13}C$-labeled protein in 95% H_2O, 5% D_2O, 50 mM phosphate buffer, pH 6.8, with 1 mM DTT.

Microtubule Preparation—Porcine brain tubulin was purified as described (5, 16) and incubated at concentrations higher than 200 μM in microtubule assembly buffer (100 mM Pipes, pH 6.9, 1 mM EDTA, 1 mM $MgSO_4$, 1 mM DTT) in the presence of 1 mM GTP at 37 °C for 5 min. After addition of 100 μM paclitaxel (Sigma), the polymerization was performed for 20 min at 37 °C. The integrity of microtubules was checked by standard negative stain electron microscopy.

NMR Spectroscopy—NMR spectra were acquired at 5 °C on a Bruker Avance 900 spectrometer equipped with a cryo-probe. Aggregation did not occur under these low temperature conditions. Three-dimensional (HA)CANNH and HNN experiments (4 scans, 1.2-s recovery delay) were collected to obtain sequence-specific assignments for the backbone of K32. NMR data were processed and analyzed using NMRPipe (17) and Sparky 3 (University of California, San Francisco). Secondary shift values were calculated as the differences between measured C^α or C′ (as obtained from a three-dimensional HNCO experiment) chemical shifts and the empirical random coil value for the appropriate amino acid type (18, 19). Using the program NMRView version 5 (20), random coil values for the primary sequence of K32 were generated. Random coil values for histidines, glutamates, and aspartates were taken from Wishart and Sykes (21), as the chemical shifts of these residues are particularly sensitive to pH and the pH in the studies by Wishart and Sykes (22) (pH 5) is more similar to the one used here (pH 6.9). Furthermore, correction factors for residues occurring in the sequence before a proline residue were also taken from Wishart and Sykes (21). To estimate the β-sheet propensity in contiguous segments of Tau, the observed C^α and C′ chemical shifts were normalized by the empirically determined secondary shift expected for that residue type in a fully β-sheet conformation (22), summed and normalized by the number of residues in the segment (23). To probe the structural consequences of binding of heparin to K32, C^α chemical shifts were measured using a three-dimensional (HA)CANNH with a K32:heparin ratio of 4:1.

Titration of K32 with heparin was carried out with uniformly ^{15}N-labeled protein containing 0.15 mM K32, pH 6.9 (100 mM Pipes, 1 mM EDTA, 1 mM $MgSO_4$, 1 mM dithiothreitol). Heparin (average molecular weight 3350, 5.8 dissaccharide subunits, charge/subunit −2.5) was from Sigma. Complex formation was monitored by recording two-dimensional ^1H-^{15}N HSQC spectra for increasing heparin concentrations (in mM) as follows: 0.0075, 0.015, 0.030, 0.074, 0.148, 0.291, 0.698, 1.304, and 2.308. As a control, an additional, single titration point was measured with a K32 solution of 67 μM with 17 μM heparin (heparin:K32 ratio of 1:4).

For Tau-MT titrations, NMR samples contained 136 μM (MT titration without sodium chloride) uniformly ^{15}N-,^{13}C-labeled and 200 μM uniformly ^{15}N-labeled K32 (titration with salt). The complex formation without salt was monitored at 5 °C for MT concentrations ($\alpha\beta$-tubulin dimers) of 15, 37.5, and 75 μM. The salt titration was performed at a MT concentration of 100 μM at 5 and 20 °C with salt concentrations 50, 100, 150, 200, and 300 mM sodium chloride.

One-bond N–H RDCs (D_{NH}) were determined by using the two-dimensional inphase-antiphase (IPAP)-HSQC sequence (24) in 300 mM sodium chloride. D_{NH} values were calculated as the difference between splittings measured in the isotropic phase and in a sample, in which K32 had been aligned in 8 mg/ml Pf1 bacteriophage (Asla, Riga, Latvia) (deuterium splitting 4.4 Hz). RDCs were not corrected for the negative gyromagnetic ratio of ^{15}N.

^{15}N R_2 and $R_{1\rho}$ relaxation rates were measured with pulse sequences based on Farrow *et al.* (25) at 5 °C on a Bruker Avance 700-MHz spectrometer. For $T_{1\rho}$, where the expected range of values is small, only two relaxation periods with 20 and 320 ms were used (26). The spin lock frequency was 1.5 kHz. For R_2 measurements, the relaxation delays were set to 20, 100, 200, and 260 ms. Relaxation times were calculated from the ratio of the signal integrals ($R_{1\rho}$) or by fitting a exponential function to the decaying signal integrals (R_2). Heteronuclear NOE values are reported as the ratio of peak heights in paired spectra collected with and without an initial period (4 s) of proton saturation during the 5-s recycle delay. Errors were calculated on the basis of the S/N ratio for each residue.

RESULTS

Backbone Assignment of K32—NMR resonances in ^1H, ^{15}N HSQC spectra of the construct K32, consisting of all four repeat motifs (R1–R4) of Tau and the two flanking regions P2 and R′ (Fig. 1), were recorded at 5 °C and pH 6.9. The resonances were sharp and showed only a limited dispersion of chemical shifts (supplemental Fig. S1), reflecting a high degree of backbone mobility and the lack of well defined secondary and tertiary structure, in agreement with circular dichroism and Fourier transform-infrared spectroscopy measurements.

To enable the study of the structure and dynamics of Tau, the assignment of the NMR resonances was required. K32 includes 198 residues with a calculated mass of 21,029 Da. Assignment of an intrinsically disordered protein of this size is not a trivial task because of the very limited chemical shift dispersion. Because of the strongly repetitive primary sequence (five types of amino acids make up more than 50% of the protein), resonances from residues located in the repeat domain were particularly affected by overlap. Moreover, the presence of 11 prolines, out of a total

Downloaded from www.jbc.org at Max Planck Inst.Biophysikalische Chemie,Otto Hahn Bibl,Pf.2841,37018 Goettingen on March 23, 2009

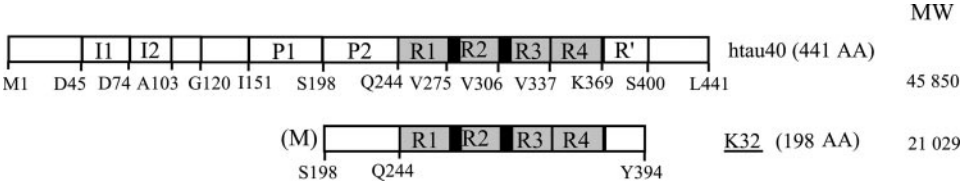

FIGURE 1. ***Bar diagrams* of full-length Tau and the fragment K32.** Full-length adult Tau (*hTau40*) contains 441 residues and can be subdivided into several domains (5). The N-terminal "projection domain" comprises residues 1–197 and does not contribute to MT binding. The C-terminal "assembly domain" contains the residues important for microtubule nucleation and stabilization. The four repeats (31 or 32 residues) are denoted as *R1–R4*. R2 (encoded by exon 10) is absent in three-repeat isoforms because of alternative splicing. The basic and proline-rich region preceding the repeats is subdivided into P1 and P2, separated by the chymotryptic cleavage site behind Tyr^{197}, which divides the projection domain and assembly domain. Fragment K32 comprises residues Ser^{198}–Tyr^{394} with a preceding methionine (198 residues), *i.e.* domains P2, R1–R4, and R′. P2 contributes a major part of the microtubule-binding affinity and contains many of the proline-directed phosphorylation sites (*e.g.* AT8 site = $S202^P + T205^P$, AT100 site = $T210^P + S212^P$, which represents the binding site of the Pin1 proline isomerase (59), and the AT180 site = $S231^P + T235^P$, which contributes to a conformational change upon proline isomerization). The C-terminal flanking region is denoted R′ because it shows weak sequence homology to the other repeats ("5th repeat"). The two hexapeptide motifs ^{275}VQIINK^{280} and ^{306}VQIVYK^{311} in R2 and R3, which are necessary for PHF formation (13), are indicated by *black rectangles*.

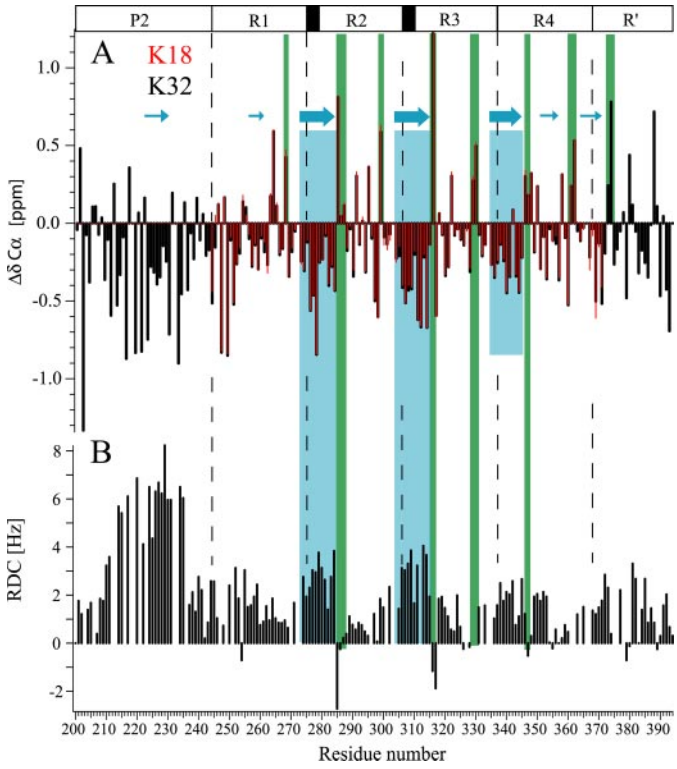

FIGURE 2. **Secondary structure propensity in K32.** *A,* secondary chemical shifts of K32 (*black*) in comparison with K18 (*red*). *B,* one-bond N–H RDCs. Regions of β-structure propensity (marked by *arrows*; *bigger arrows* indicate stronger β-structure propensity) are identified by negative values extending over several residues, which are also highlighted by *blue boxes*. *Green boxes* indicate residues with turn character as suggested by positive secondary chemical shifts and negative RDCs. Repeat boundaries are indicated by *vertical dashed lines*.

of 46 residues (almost 25%) in the basic region P2, further complicated the assignment. These complications could be overcome by the use of high resolution three-dimensional (HA)CANNH and three-dimensional HNN experiments (supplemental Fig. S2), in combination with the previously determined assignment of the isolated four repeats (on referred to below as construct K18) (27). No resonances for Ser^{198} and Ser^{199} were detectable. This could be due to enzymatic cleavage of these N-terminal residues or line broadening caused by the conformational flexibility of the N terminus. In addition, residues Gly^{272}, Gly^{303}, Gly^{334}, and Gly^{366} (surrounded by two glycines in the sequence motif PGGG, which occurs at the C-terminal end of each repeat region) and Gly^{304}/Gly^{335} could be identified in the spectra, but their unambiguous assignment was not possible because of high resonance overlap. In total, about 95% of K32 residues were assigned unambiguously (prolines excluded). The achieved assignment constitutes ~45% of the sequence of hTau40, the longest Tau isoform in the human brain (441 residues).

Comparison with the assignment of K18 showed that the positions of peaks belonging to the four repeats remained largely unaffected by the presence of additional flanking regions (data not shown). Moreover, with the exception of the 10 N-terminal residues of K18, signal intensities within the repeat domain were not significantly altered. This underlines the character of Tau as an intrinsically disordered protein.

Secondary Structure Propensity in K32—NMR chemical shifts, in particular of C^α atoms, are very sensitive probes of secondary structure both in globular and intrinsically disordered proteins (22, 28). These shifts show small but distinct deviations from random coil values for K32 (Fig. 2). Several continuous stretches (containing 7–11 residues) with negative secondary chemical shifts were observed, in particular Lys^{274}–Leu^{284} (R1/R2), Ser^{305}–Asp^{315} (R2/R3), and Gln^{336}–Asp^{345} (R3/R4). Continuous stretches of negative secondary chemical shifts indicate a propensity for β-structure. According to a quantitative analysis of the C^α secondary chemical shifts, the β-structure-like conformations are populated 22, 25, and 19% of the time for residues Gly^{273}–Leu^{284}, Gly^{304}–Leu^{315}, and Gly^{333}–Asp^{345}, respectively. These elements of β-structure are located at the beginning of R2, R3, and R4. The corresponding region in repeat 1 does not show a strong propensity for β-structure, most likely because of the presence of proline residues Pro^{247} and Pro^{251}. Residual β-structure was also observed for residues Val^{256}–Ser^{262} and Gln^{351}–Leu^{357}, which are located roughly in the center of repeats R1 and R3. In the R′, the region downstream of the repeat motifs, which shows only a weak sequence homology to the repeats, no strong tendency to populate either helical or β-structure was detected. On the other hand, quite large negative secondary chemical shifts were present in the proline-rich region P2, with Pro^{223}–Arg^{230} forming a continuous stretch. The pattern of C′ secondary chemical shifts was very similar to that observed for C^α (supplemental Fig. S3) indicating that either C^α or C′ chemical shifts can be used for detection of transient structure in unfolded proteins. Comparison of K32 with K18, *i.e.* the construct in which the two flanking domains are missing, shows an almost identical pattern of secondary chemical shifts for residues Ala^{246}–Ile^{371} demonstrating that the flanking regions do not significantly

Downloaded from www.jbc.org at Max Planck Inst.Biophysikalische Chemie,Otto Hahn Bibl,Pf.2841,37018 Goettingen on March 23, 2009

affect the secondary structure propensity in the repeat domain of Tau.

To obtain further insight into the secondary structure propensity, we measured one-bond N-H residual dipolar couplings (RDCs) in K32, which had been partially oriented in a Pf1 bacteriophage alignment medium. In an anisotropic environment, like magnetically oriented Pf1 phage, the large one-bond internuclear dipolar interactions no longer average to zero. In contrast to the bell-like smooth distribution of dipolar couplings, which is expected for random flight chains (29), a very specific distribution of positive and negative couplings was observed for K32 (Fig. 2*B*). In the region R1–R4 two stretches of high positive RDC values were evident, ^{274}KVQIINKKLDL^{284} and ^{306}VQIVYKPVD^{314}. These regions correlate well with the elements of high β-structure propensity at the beginning of R2 and R3, as identified by NMR secondary chemical shifts (Fig. 2). Note that the β-regions at the beginning of R2 and R3 encompass the two PHF-promoting hexapeptide motifs (13), whereas the β-region in R4 overlaps with the "module B" motif that determines the packing of Tau into twisted PHFs (30). The regions with large RDCs end with residues displaying negative RDCs: Lys^{254}, Ser^{285}, Asn^{286}, Ser^{316}, Lys^{317}, Gly^{326}, Ile^{328}, Lys^{347}, Gly^{355}, Arg^{379}, Glu^{380} and Gly^{389}. The same residues show positive secondary chemical shifts, and we previously proposed that they are involved in turn structures (27). In the proline-rich region P2, particularly large and positive RDC values were found. The RDC magnitude for residues Ser^{214}–Ser^{235}, a region in which eight prolines are located, is about twice the size than in the rest of the protein.

In contrast to RDCs, which are influenced by both structure and dynamics, ^{15}N spin relaxation times can directly probe the motion of the protein backbone in a site-specific manner (31). ^{15}N $R_{1\rho}$ and R_2 spin relaxation rates are sensitive to motions of the backbone occurring on the pico- to nanosecond as well as micro- to millisecond time scale. The ^{15}N on-resonance $R_{1\rho}$ rates observed in K32 at 5 °C follow a smooth bell-like distribution with an average value of 3.7 Hz, underlining the character of Tau as a natively unfolded protein (Fig. 6). At the termini the relaxation rates are reduced, in agreement with an increased flexibility. Some residues such as Ile^{308}–Lys^{317} show slightly higher $R_{1\rho}$ values, reporting on motional restrictions in these regions. On the other hand, heteronuclear steady-state ^{15}N NOE values were all close to zero (supplemental Fig. S4), indicating that abundant pico- to nanosecond dynamics occur along the polypeptide chain of K32, and fully formed regular secondary structure elements are not present. In contrast to $R_{1\rho}$ rates, R_2 spin relaxation times are also affected by chemical exchange. Thus, a difference plot between R_2 and $R_{1\rho}$ rates identifies residues that exchange between multiple conformations in solution. In K32, above average chemical exchange contributions are most evident for residues Gly^{201}–Ser^{210}, Ser^{237}–Ser^{241}, Gly^{271}, Lys^{290}–Gly^{292}, Lys^{298}, Gly^{302}, Val^{309}–Lys^{321}, Gly^{323}, Gly^{333}, Asn^{368}, and Phe^{378}.

Interaction of Tau-K32 with the PHF Inducer Heparin—NMR signals of backbone amides constitute excellent probes of complex formation (32), providing maps of interaction interfaces. We were particularly interested in the interaction of Tau with its physiological target microtubules, and with the polyanion heparin that induces the formation of Alzheimer-like PHFs. The binding of heparin to K32 was monitored by two-dimensional ^{1}H-^{15}N HSQC spectra. This allows one to identify the residues that are important for the binding to polyanions. At high heparin concentrations chemical shift changes of some residues were accompanied by a decrease of the intensity of their signals, indicating chemical shift exchange intermediate on the NMR time scale. The chemical shift perturbation experiments showed the strongest shifts in the following regions (Fig. 3*A*): Thr^{217}–Leu^{253} (most pronounced for ^{243}LQTA^{246}), ^{275}VQIINKKLDLSN^{286}, ^{298}KHV^{300}, ^{372}ETHKLTFRENAK^{383}. The chemical shift differences correlate very well with the signal intensity ratios (residue intensity of spectrum with ligand: residue intensity of the unperturbed spectrum of unbound protein) of these spots (Fig. 3*B*). For strongly shifting residues the intensity ratios were generally below 70% of their original values. In the regions around Lys^{225}, Thr^{244}, Asn^{279}, and Thr^{373}, the signal intensity was reduced even down to about 40%, indicating that these residues are strongly involved in exchange processes intermediate on the NMR time scale. Besides the binding sites deduced from the chemical shift changes, ^{212}TPSLP^{216}, ^{306}VQIVYKPV^{313}, and ^{325}LGNIHHK^{331} were identified as being important for the heparin binding by exchange broadening (Fig. 3*B*). In most regions of K32 strongly affected by heparin, positively charged residues are present as follows: Arg^{211}, Arg^{242}, Lys^{280}, Lys^{281}, Lys^{298}, His^{299}, Lys^{311}, His^{329}, His^{330}, Lys^{331}, His^{374}, Lys^{375}, and Arg^{379}. This indicates that the binding to heparin is of electrostatic nature. Because of the presence of two lysine residues and one arginine, charge-charge interactions might also occur with the stretch ^{224}KKVAVVR^{230}, but in this case a hydrophobic contribution is possible as well.

To probe the structural impact of binding of heparin to Tau, we determined the C^{α} secondary chemical shifts of Tau in presence of heparin (Tau:heparin 4:1). NMR chemical shifts can be measured with high accuracy such that even minute changes in secondary structure can be detected. However, the C^{α} chemical shifts of K32 with and without heparin were virtually identical (supplemental Fig. S5), indicating that heparin binding does not induce a significant increase in β-structure under these conditions.

Tau-Microtubule Interactions and the Jaws Model—The binding of K32 to MTs was characterized using NMR chemical shift perturbation as described (27), where two-dimensional ^{1}H-^{15}N HSQC spectra of K32 were recorded in the presence of increasing amounts of taxol-stabilized MTs. The influence of temperature was probed by performing NMR titrations at 5 and 20 °C. As shown previously, taxol-stabilized microtubules are stable at 5 °C for several hours, sufficient for the time course of the NMR experiment, and Tau binds to them (27). The overall signal intensity in two-dimensional ^{1}H-^{15}N HSQC experiments decreases rapidly at high MT concentrations, indicative of an increasing amount of K32 strongly bound to MTs. Because of very fast relaxation, the NMR signals of MT-bound K32 are no longer observable. Nevertheless, continuous chemical shift changes and additional exchange-induced broadening of specific regions of K32 were observed with increasing MT concentrations. It is immediately apparent from Fig. 4 that both the

Downloaded from www.jbc.org at Max Planck Inst.Biophysikalische Chemie,Otto Hahn Bibl,Pf.2841,37018 Goettingen on March 23, 2009

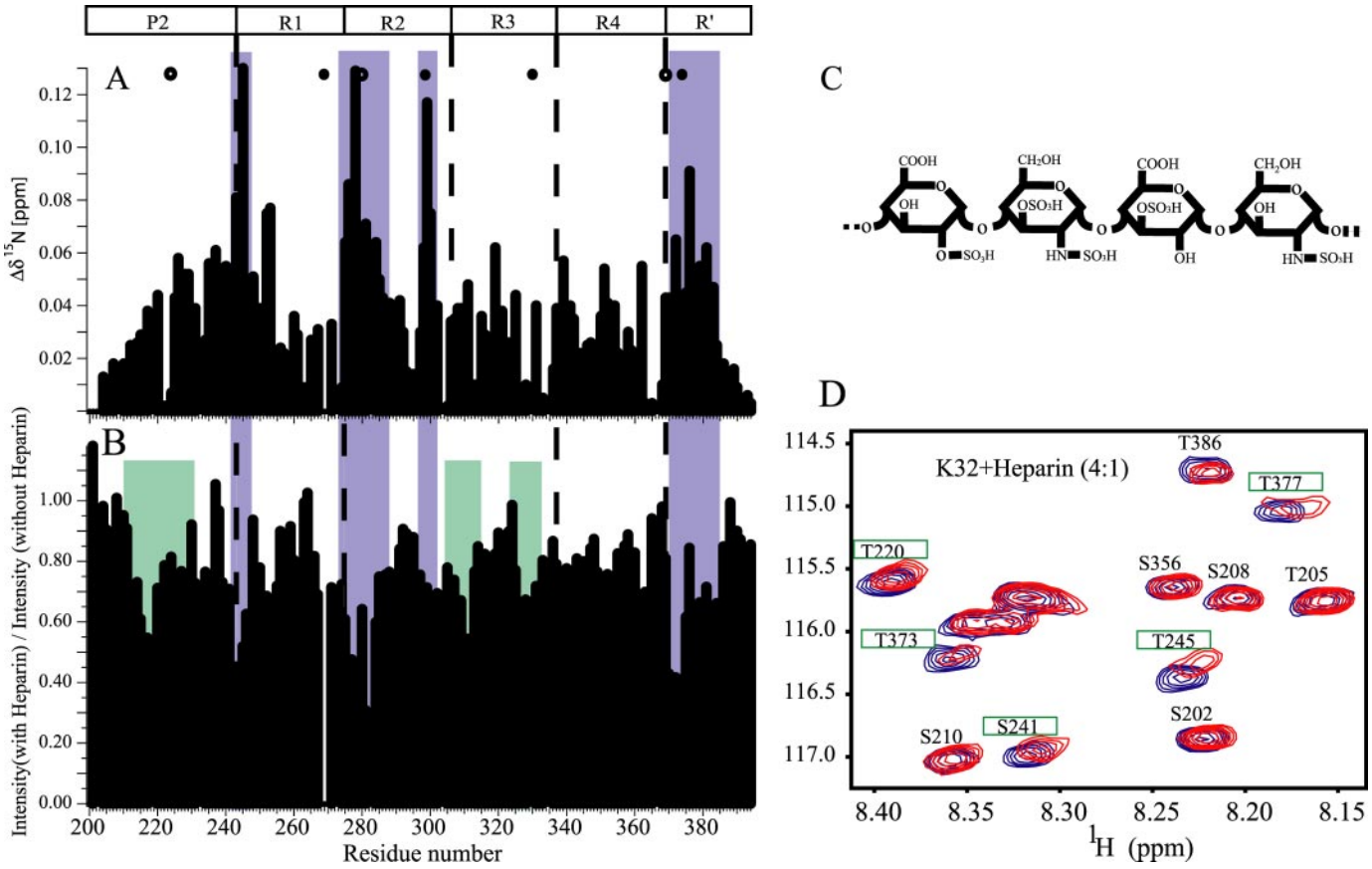

FIGURE 3. **Tau-heparin interaction.** *A,* ^{15}N chemical shift differences; *B,* ratio of signal intensity of the protein in the heparin-bound state and in solution without heparin. K32 (67 μM) with heparin (17 μM) at 5 °C and pH 6.9. *Blue boxes* indicate the strongest binding sites identified on the basis of chemical shift differences. *Green boxes* highlight binding sites only visible by comparison of intensities. Lys-Lys dyads are indicated by *open circles* and Lys-His dyads by *filled circles. C,* structure of heparin. *D,* overlay of the ^{1}H, ^{15}N HSQC spectra of K32 without (*blue*) and with heparin (*red*). Some strongly shifting residues are highlighted with *green boxes.*

P2- and the R′-flanking regions, as well as the repeat domain itself, strongly contribute to the interaction with microtubules. The strongest chemical shift changes, pointing to a strong involvement into the MT-binding process, were observed for residues ^{225}KVAVVRT^{231} in domain P2, ^{240}KSRLQTAPV^{248} in domain R1, ^{275}VQIINKKLDLS^{285} and ^{297}IKHV^{300} in R2, and ^{370}KIETHK^{375} in R′. The strong contribution of the flanking domains is consistent with their role as microtubule-targeting domains (jaws). In addition, however, other isolated residues were strongly perturbed in the presence of MTs. The location of the jaws of MT binding became clearer, when the reduction in ^{1}H-^{15}N HSQC signal intensities caused by addition of MTs was taken into account (Fig. 4*B*). For most of the residues from Leu^{215} to Lys^{331}, the intensity was reduced to below 40% at a K32:MT ratio of ~2:1. Particularly low signal intensities were observed for residues ^{222}EPKKVAVVRT^{231}, ^{275}VQIINKKLDLSNVQSK^{290}, ^{306}VQIVYKPVDLSKVTSK^{321}, and ^{377}TFREN^{381}. Both signal intensity ratios and chemical shift changes indicate that repeat R4 and the outermost residues in K32, Gly^{200}–Ala^{209} and Thr^{386}–Tyr^{394}, do not significantly bind to MTs.

At 20 °C, the overall magnitude of chemical shift changes induced by the presence of MTs was decreased (Fig. 4*A*). In particular, the chemical shift changes of residues ^{240}KSRLQTAPV^{248}, ^{275}VQIINKKLDLS^{285}, and ^{370}KIETHK^{375} were less pronounced. In comparison to the results at 5 °C, large chemical shift changes remained for ^{225}KVAVVRT^{231} and ^{297}IKHV^{300}. Signal intensity ratios between the free and the MT-bound state of K32 were less informative than at 5 °C. Overall, the reduction in signal intensity in the MT-bound state was lower than at 5 °C, and signal intensities were more uniform along the whole K32 sequence (data not shown).

The binding of Tau to MTs occurs in two structurally and kinetically distinct steps, comprising a first binding phase with low stoichiometry but tight binding (K_d ~0.1 μM) and a second phase of weaker affinity but higher and nonsaturable stoichiometry (33). Solution NMR spectroscopy cannot detect Tau molecules that are fully bound to MTs because of the large molecular weight of the complex and the accompanying fast signal decay. To test if the binding sites identified by the NMR titrations of K32 with MT are characteristic also for the strong primary binding of Tau to MTs, we repeated the K32-MT titration at increased ionic strengths. Previous studies have shown that in the presence of sodium chloride, the MT-binding strength of Tau is reduced and the weaker, nonsaturable binding is strongly attenuated (34). In agreement with these results, the addition of 100 mM NaCl to the Tau-MT solution (K32:MT = 2:1) increased the average ratio of signal intensities to about 80% (data not shown). A further increase to 300 and 600 mM NaCl raised the average signal intensity ratio to a maximum value of 85%. This indicates that at 300 mM NaCl, the off-rate is

Downloaded from www.jbc.org at Max Planck Inst.Biophysikalische Chemie,Otto Hahn Bibl,Pf.2841,37018 Goettingen on March 23, 2009

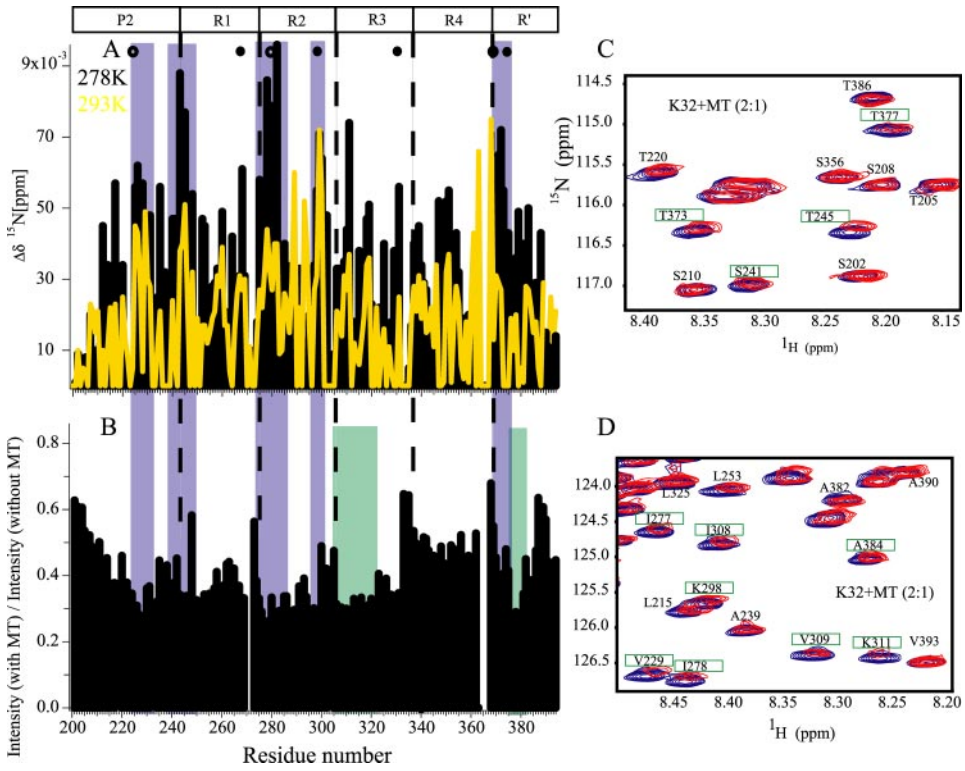

FIGURE 4. **Binding of Tau to microtubules.** *A,* ^{15}N chemical shift differences. K32 (136 μM) with MT (75 μM) at 5 °C (*black bars*) and K32 (200 μM) with MT (100 μM) at 20 °C (*yellow curve*). Lys-Lys dyads are indicated by *open circles* and Lys-His dyads by *filled circles. B,* ratio of intensities of signals of the protein in the MT-bound state and in the free state. Binding sites identified by reduced intensities are indicated by *green boxes. C* and *D,* overlay of the ^{1}H, ^{15}N HSQC spectra of K32 without (*blue*) and with MT (*red*). Some residues that experience a strong change in chemical shift or have a significantly reduced signal intensity are highlighted with *green boxes.*

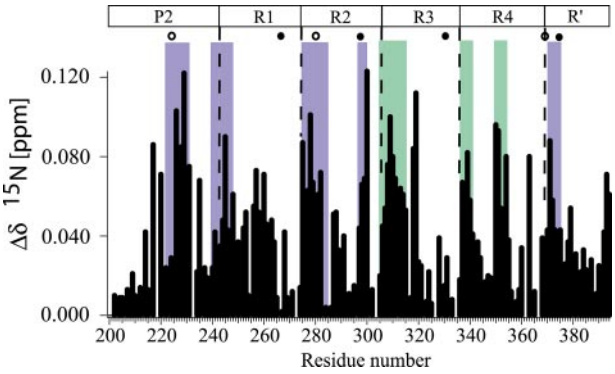

FIGURE 5. **Influence of ionic strength on Tau-MT interaction.** ^{15}N chemical shift differences in K32 (200 μM) in the presence of 100 μM MT and 300 mM sodium chloride at 5 °C, pH 6.9. Binding sites observed in the absence of salt are highlighted by *blue boxes*, whereas spots with stronger shifts in presence of sodium chloride are indicated by *green boxes*. Lys-Lys dyads are indicated by *open circles* and Lys-His by *filled circles.*

sufficiently increased, such that most K32 molecules now contribute to the NMR signal. Fig. 5*A* shows the chemical shift changes induced in K32 upon addition of MTs at 5 °C in the presence of 300 mM NaCl. The same residues that show large chemical shift changes without NaCl were also strongly affected at 300 mM NaCl. Because of the higher ionic strength, the interactions with the positively charged binding hot spots of K32 were weakened. The most strongly shifting resonances were now located in the stretch ^{225}KVAVVRT^{231} in the upstream flanking domain, suggesting that there is a hydrophobic MT-binding contribution originating from this region. In addition, signals from residues ^{337}VEVK^{340} and ^{350}VQSKI^{354} were more strongly affected than in the absence of sodium chloride. Taken together, the high salt titration of K32 with MTs demonstrates that the binding profile identified by our NMR studies reports on the primary, strong binding of Tau to microtubules. Note that at 20 °C and in the presence of 300 mM NaCl no MT binding was detected anymore, as judged by NMR chemical shifts and signal intensity ratios (data not shown).

DISCUSSION

Tau is an interesting protein in several respects. As an intrinsically disordered protein, it challenges the paradigm that a folded structure is necessary for function. Tau is a major microtubule-associated protein involved in the formation of axons and stabilization of microtubules as tracks for axonal transport. In the form of paired helical filaments, Tau constitutes one of the hallmarks of Alzheimer disease. Therefore, key questions concerning the structure and function of Tau protein include the following. What are the binding sites of Tau to microtubules? How is the aggregation of Tau into PHFs facilitated? To address some of these questions we investigated a 198-residue fragment (K32), comprising the four repeat motifs and the two flanking basic domains P2 and R′ (Fig. 1). The repeat domain forms the core of the microtubule-binding domain and also the core of PHFs (3, 9). However, maximal binding of Tau to microtubules requires the two flanking regions P2 and R′. This was interpreted in terms of jaws of the Tau-microtubule interaction (6).

Residual β-Structure in Repeat Domain and Random Coil Structure in Flanking Domains—Backbone resonance assignment of K32 is challenging, because of the small chemical shift dispersion, the repetitive nature of the repeat domain, and the large number of prolines in domain P2. We were able to assign 95% of non-proline residues of K32, equivalent to 40% of all residues of full-length Tau. This extends and is complementary to recent work of Lippens and co-workers (36) who reported a partial assignment of Tau. In this study, the unambiguously assigned residues (~30–40%) were mainly located in the acidic N-terminal header domain (residues 1–120) and in the C-terminal tail domain (residues 390–441), whereas only a few residues in the K32 region could be assigned unambiguously. Thus, our assignment of K32 was essential for the investigations reported here and will be useful for future studies of Tau, such as the structural consequences of phosphorylation or the influence of FTDP-17 mutations.

Downloaded from www.jbc.org at Max Planck Inst.Biophysikalische Chemie,Otto Hahn Bibl,Pf.2841,37018 Goettingen on March 23, 2009

Assignment of backbone chemical shifts in proteins gives access to detailed information on secondary structure. The difference between experimental chemical shifts and random coil values, which are specific for the sequence of the protein under investigation, allows site-specific detection of even small propensities for helical or β-structure. In K32, the initial stretches of R2, R3, and R4 have the most pronounced β-sheet propensity, with average values of 22, 24, and 19% for residues Gly^{273}–Leu^{284}, Gly^{304}–Leu^{315}, and Gly^{333}–Asp^{345}, respectively. This agrees well with other biochemical and structural studies showing that these regions are involved in the assembly of PHFs and their molecular packing (13, 30). In addition, residues Lys^{224}–Arg^{230}, Val^{256}–Ser^{262}, Gln^{351}–Leu^{357}, and Val^{363}–Glu^{372} preferentially populate extended structures (Fig. 2 and Fig. 7). No α-helical structure was detected in the repeat domain in this study. This is contrary to other NMR studies of Tau-derived fragments that were performed, however, in the presence of helix-inducing agents such as trifluoroethanol or SDS (37–39). In addition, no strong tendency to populate α-helical or β-structure was detected in the regions flanking the repeat domain. In the N-terminal P2 domain (Ser^{198}–Leu^{243}), this is most likely because of the large number of proline residues. This feature, combined with the presence of many residues with comparably large negative secondary chemical shifts (Fig. 2*A*), hints to a tendency for formation of a polyproline helix in this region. Indeed, phosphorylation at residues Thr^{231}, Ser^{235}, and Ser^{237} seems to induce polyproline helix conformations for residues Val^{229}–Ser^{238} (40).

Residual dipolar couplings can be measured in a weakly aligned macromolecule, for which the large one-bond internuclear dipolar interactions no longer average to zero (41, 42). RDCs are exquisitely sensitive to bond vector orientation and offer many new opportunities in NMR studies of proteins in solution. In highly dynamic systems, such as intrinsically disordered proteins, RDCs define local conformational behavior as well as long range order (43). In the repeat domain of Tau, large RDCs correlate with regions that preferentially populate β-structure as indicated by NMR chemical shifts. In particular, in the two hexapeptide motifs at the beginning of repeats R2 and R3, which are crucial for aggregation of Tau into PHFs, RDCs are about twice the size than in the rest of the repeat domain (Fig. 2*B*). The C-terminal ends of these regions are characterized by positive secondary chemical shifts and negative RDCs. This suggests the formation of turns at these sites. The largest positive RDCs were observed, however, for residues Ser^{214}–Ser^{235} in the center of the proline-rich domain P2. For the analogous case of α-synuclein (the protein that irreversibly aggregates in the course of Parkinson disease), we have shown previously that large RDCs in the C-terminal domain were because of an increased rigidity of the protein backbone, which was induced by long range interactions (44). Thus, long range interactions within K32 might be responsible for the increased magnitude of RDCs in the P2 domain. Alternatively, the increased RDC magnitude of Ser^{214}–Ser^{235} might be due to the large number of prolines in this region, which make the backbone more rigid. Comparison of chemical shifts and signal intensity ratios between K32 and K18 (the construct lacking the flanking P2 and R′ domains), steady-state NOE values, and ^{15}N transverse relaxation rates do not provide any evidence for a folding back of P2 or R′ on the repeat region. This, however, does not exclude very transient interactions. To probe for transient long range interactions, several single cysteine mutants of K32 would be required, to which a paramagnetic nitroxide radical can be specifically attached. This work is in progress. Noteworthy, the strongly increased RDC magnitude of Ser^{214}–Ser^{235} is not accompanied by above average ^{15}N $R_{1\rho}$ rates or steady-state NOE values, indicating that motions in the nano- to microsecond time scale (toward which $R_{1\rho}$ rates are not sensitive) are reduced in this region.

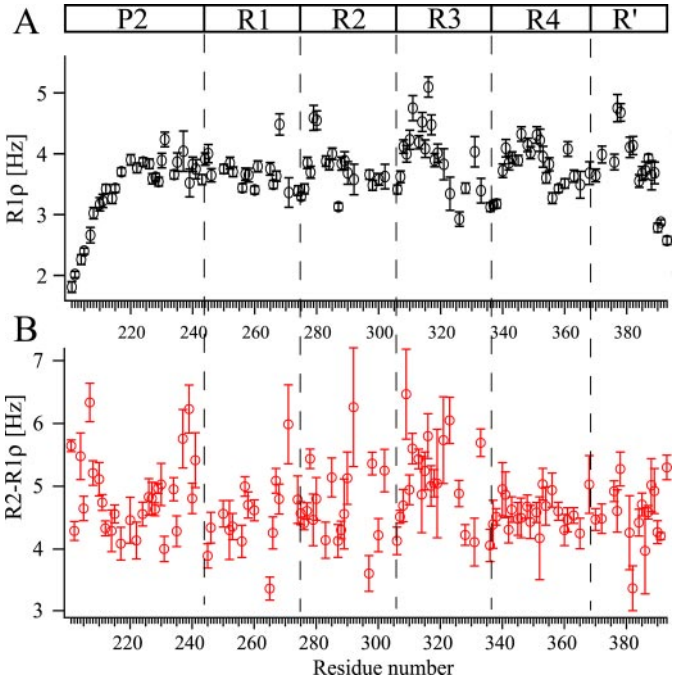

FIGURE 6. **Intrinsic dynamics of K32.** *Top,* ^{15}N R1ρ spin relaxation rates of K32 (300 μM) at 5 °C. *Bottom,* difference between R2 and R1ρ rates, which probes chemical exchange occurring on the micro- to millisecond time scale.

To probe the intrinsic dynamics of Tau, we measured ^{15}N transverse spin relaxation rates. In particular, the glycine residues Gly^{201}, Gly^{271}, Gly^{292}, Gly^{302}, Gly^{323}, and Gly^{333} were strongly affected by chemical exchange (Fig. 6), suggesting that they function as flexible linkers between more rigid parts of the molecule. Gly^{271}, Gly^{302}, and Gly^{333} are part of the PGGG motifs just upstream of the hexapeptides in the repeats. On the basis of secondary chemical shifts, we previously suggested that these residues form turns. In addition, pronounced chemical exchange was observed for the stretch Val^{309}–Lys^{321}, which encompasses the hexapeptide motif of R3. This region has the strongest propensity to form β-structure according to secondary chemical shifts, suggesting that the hexapeptide motif of R3 exchanges between a random coil conformation and β-structure in solution.

In the fibrillar state, the repeat domain of Tau assumes the characteristic cross-β-structure with a high content of β-strands (45–47). By NMR secondary chemical shifts, we could clearly identify several regions in K32, primarily located in the repeat domain, with a pronounced tendency to populate β-structure. Therefore, it is tempting to speculate that these regions serve as seeds of aggregation. Dimer formation as the

Downloaded from www.jbc.org at Max Planck Inst.Biophysikalische Chemie,Otto Hahn Bibl,Pf.2841,37018 Goettingen on March 23, 2009

initial step of aggregation might be initiated by intermolecular contacts between the regions of high β-structure propensity. The intermolecular interaction will stabilize the β-structure and ultimately convert these parts into β-sheets in PHFs. This idea is supported by the prediction of aggregation hot spots using the program Zyggregator (48). It predicts three hot spots of aggregation for the Tau peptide Asn^{265}–Glu^{338} as follows: residues Lys^{280}–Val^{287}, Val^{305}–Lys^{311}, and Gly^{335}–Lys^{340}. In addition, based on experimental aggregation propensities derived from Tau-related peptides, the two hexapeptides in the beginning of repeats R2 and R3 (^{275}VQIINK^{280} and ^{306}VQIVYK^{311}), ^{226}VAVVR^{230}, and ^{392}IVYK^{395} are predicted to have high aggregation propensities (49). These stretches correlate well with the regions of experimentally determined β-structure propensity.

Regions Flanking the Repeat Domain Are Involved in Binding to PHF-inducing Polyanions—Because Tau is a highly soluble protein, it normally resists aggregation; however, aggregation can be enhanced by different polyanions, presumably because they overcome the charge repulsion of the cationic Tau molecules. Examples are sulfated glycosaminoglycans, heparin, RNA, and acidic peptides resembling the C-terminal domain of tubulin (50–52). It was therefore of interest to determine which residues in Tau are involved in the interaction with microtubules and polyanions such as heparin.

Previously, we have shown that heparin binds to the hexapeptide motifs in the repeat domain, as well as to positively charged patches such as the KK motif at the beginning of R2 (^{280}KK^{281}) and the KH (^{267}KH^{268} and ^{298}KH^{299}) or HHK (^{329}HHK^{331}) motifs near the end of the repeats R1, R2, and R3. These studies were performed on K18, a 130-residue fragment of Tau that just comprised the repeat domain (27). These studies show that heparin binds to the same positively charged patches in the repeat domain, even when the two flanking regions P2 and R′ are present. In particular, the fact that the hexapeptide VQIINK in the beginning of repeat 2, which is important for aggregation of Tau into PHFs, preferentially populates β-structure and binds to the polyanion heparin also in K32 underlines the hypothesis that polyanions enhance aggregation of Tau by reducing electrostatic repulsion between different Tau molecules. In contrast to a recent study (53), we could not detect any increase in β-structure in Tau upon addition of heparin. Our measurements were performed with a 4:1 ratio of Tau:heparin, which was described as optimum for induction of Tau aggregation by heparin (54). Besides a different Tau:heparin ratio, Sibille *et al.* (53) used full-length Tau and a specific low molecular weight version of heparin.

Here we show that both flanking domains, P2 and R′, are also involved in the interaction with heparin (Fig. 3). Most notably, Lys^{224}–Arg^{230}, the only region outside of the repeat domain for which NMR secondary chemical shifts indicated a propensity to form β-structure, binds to heparin. Similar to the hot spot of aggregation in the beginning of repeat 2 (^{274}KVQINNK^{280}), the ^{224}KKVAVVR^{230} sequence contains two adjacent lysine residues separated from a third positively charged residue (Arg^{230}) by several uncharged amino acids. Therefore, the mechanism of interaction with heparin might be similar, and regions outside of the repeat domain may play a role in aggregation of Tau into PHFs.

The Jaws of the Tau-Microtubule Interaction—The microtubule-associated protein Tau is a critical regulator of diverse microtubule functions (5, 55, 56). The repeat domain with its four repeats is essential for microtubule assembly; however, in the absence of the two flanking regions P2 and R′, the repeat domain binds only weakly to microtubules. The flanking domains, on the other hand, bind to microtubules even in the absence of the repeats. This has led to the proposition of the jaws model of Tau whereby the regions flanking the repeats are considered as targeting domains, responsible for positioning Tau on the microtubule surface, and the repeats that act as catalytic domains for microtubule assembly (5, 6). The aim of this study was to provide a structural view of the residues located in the flanking regions, which are important for binding of Tau to microtubules. The 198-residue fragment K32, which consists of the repeats and the flanking domains P2 and R′, is well suited for this aim, as it captures the full microtubule binding and assembly activity of the longest Tau isoform, hTau40, in the human brain.

We used solution-state NMR to identify which residues contribute to the jaws of the Tau-microtubule interaction. Solution-state NMR can only observe molecules that are rapidly tumbling in solution, excluding the direct observation of Tau molecules completely bound to MTs. Nevertheless, information about the residues important for binding to microtubules can be obtained when the exchange between the fully bound form and the free state is sufficiently fast, such that conformational characteristics of the bound state are transferred to the soluble, unbound protein. Here, we investigated changes in NMR chemical shifts and signal intensity ratios for increasing amounts of MTs. The observed signal is an average of the resonances originating from the unbound and bound forms of Tau. The magnitude of chemical shift changes will depend on the chemical environment in the bound state and the concentration of the bound species. The latter depends on the rates with which Tau binds and detaches from MTs. In addition, residues that are involved in the binding process will be affected by conformational exchange, potentially affecting the NMR signal intensity of these residues. Therefore, we have two tools available, NMR chemical shift and signal intensity changes that allow identification of the binding sites of Tau to MTs. These two tools show that the binding behavior of Tau to heparin and taxol-stabilized MTs is similar (Fig. 4 and Fig. 7). Within the repeats the same residues that were identified as binding sites on the basis of an NMR titration of K18 (the construct comprising only the repeats) with MTs (27) are important for binding of K32 to MTs. In particular, residues ^{275}VQIINKKLDLS^{285} (comprising the hexapeptide in the beginning of repeat 2) show large chemical shift changes, in agreement with biochemical analyses that reported a strong reduction of MT binding affinity upon mutation of Lys^{274} or Lys^{281} to alanine (57). In addition, clusters of positive charges upstream of the PGGG motifs at the end of repeats 1, 2, and 3 contribute to the MT binding, thereby providing attachment points for these repeats to tubulin. Repeat 4, on the other hand, does not significantly contribute to MT binding (Fig. 4).

Downloaded from www.jbc.org at Max Planck Inst.Biophysikalische Chemie,Otto Hahn Bibl,Pf.2841,37018 Goettingen on March 23, 2009

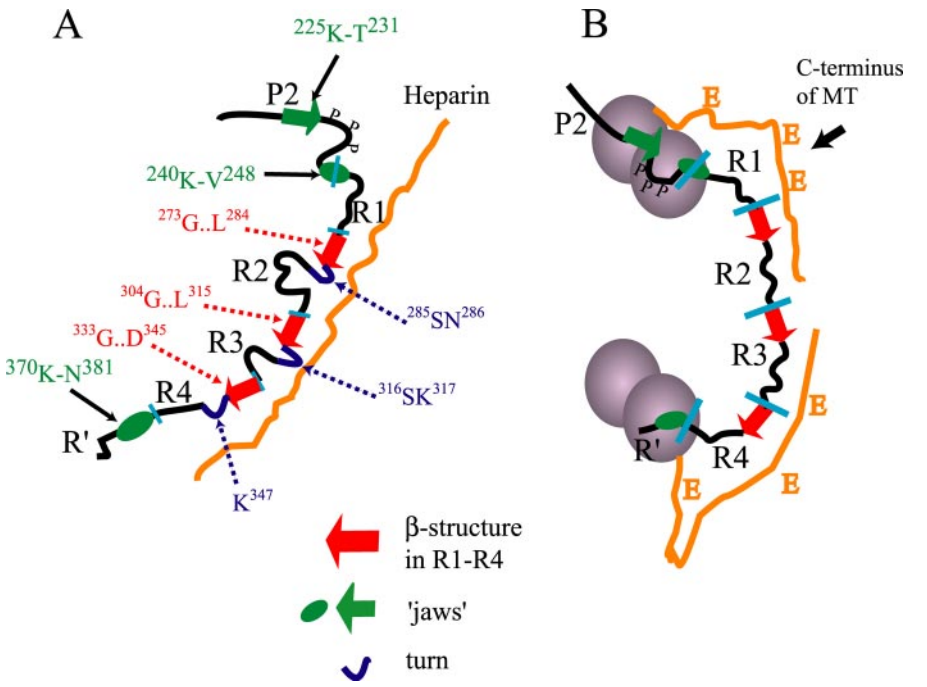

FIGURE 7. **Transient structure and microtubules and polyanion-binding properties of K32.** *A,* regions that transiently populate *β*-structure are indicated by *red arrows* (within the repeat region) and *green arrows* (in the flanking domains). Turns are highlighted in *blue.* Domain boundaries are marked by *light blue bars.* The interaction with heparin is depicted schematically. *B,* Tau binds to the Glu-rich C terminus of MTs via specific (*green ellipses* and *green arrow*) regions located in the P2 and R′ regions of Tau. The negative charges of the Glu residues function like polyanions and shield repulsive positive charges.

For high affinity binding of Tau to MTs, the regions flanking the repeats are required (5). Our NMR studies show that ^{225}KVAVVRT^{231} and ^{240}KSRLQTAPV^{248} in the proline-rich domain and ^{370}KIETHKLTFREN^{381} in the region downstream of the repeats are binding sites for both heparin and microtubules (Fig. 7). In the proline-rich domain the most strongly affected residues are ^{226}VAV^{228} and ^{243}LQT^{245}. In agreement with the NMR data, deletion analysis mapped the microtubule binding activity of the proline-rich region to residues Lys^{224}–Asn^{255} and in particular to the stretch ^{225}KVAVVRT^{231}. Moreover, site-directed mutagenesis indicated that Lys^{224}, Lys^{225}, and Arg^{230} are important for MT binding and assembly (58). It is noteworthy that the region ^{225}KVAVVRT^{231} is conserved between Tau and two other microtubule-associated proteins MAP-2 and MAP-4 (58). Interestingly, the two motifs 225–231 and 240–248 flank the motif ^{231}TPPKSP^{236} that contains two major phosphorylation sites (by GSK3*β* and/or cdk5) and the residue Pro^{232}, whose isomerization by Pin-1 is important for the accessibility to phosphatases (59).

Over 30 phosphorylation sites have been identified in Tau, for many of which the level of modification is elevated in Alzheimer disease (60–62). Prominent sites are located in the flanking domains, *e.g.* Ser^{199}, Ser^{202}, Thr^{205}, Thr^{212}, Ser^{214}, Thr^{231}, and Ser^{235} before the repeats, Ser^{396}, Ser^{404} and others after the repeats (not contained in K32). The major sites within the repeats are located in the *KXGS* motifs, *i.e.* Ser^{262}, Ser^{293}, Ser^{324}, and Ser^{356}. These sites are phosphorylated by the kinase MARK, which results in the detachment of Tau from microtubules (35). Ser^{262}, Ser^{293}, and Ser^{324} are separated by only four residues from the charged patches at the C-terminal end of repeat 1, 2, and 3, and Thr^{231} is right in the middle of the MT binding region in the proline-rich domain. Thus, phosphorylation might lead to intramolecular charge neutralization of the positive spots required for MT binding. The required bending in the backbone would easily be possible because of the high conformational flexibility of Tau. Alternatively or in combination, phosphorylation can induce other conformational changes, such as the stabilization of a polyproline II helix. Indeed, CD and NMR data on peptides derived from the proline-rich region of Tau suggest that phosphorylation induces a polyproline II helix for residues Val^{229}–Ser^{238} (40). Residues Val^{229}–Ser^{238} are located between the two MT-binding elements of the proline-rich domain (^{225}KVAVVRT^{231} and ^{240}KSRLQTAPV^{248}) and include the Pin1 target site of proline isomerization that is a major regulator of the conformation of Tau. Thus, stabilization of a polyproline II helix in this region would increase the distance between the two MT-binding sites, such that they no longer fit to their interaction sites on the MT surface.

In conclusion, we have provided a detailed view of the structural properties and of the sites of interaction with microtubules and polyanions of a fragment of Tau, which contains the full microtubule binding and assembly activity of the longest Tau isoform, hTau40, in the human brain. It will be interesting to see how genetic mutations and phosphorylation affect the hot spots of aggregation and the jaws of the Tau-microtubule interaction. These studies are currently in progress.

Acknowledgments—We thank Sabrina Hübschmann for excellent technical assistance and Dr. Eva-Maria Mandelkow for advice throughout this work.

REFERENCES

1. Garcia, M. L., and Cleveland, D. V. (2001) *Curr. Opin. Cell Biol.* **13,** 41–48
2. Cassimeris, L., and Spittle, C. (2001) *Int. Rev. Cytol.* **210,** 163–226
3. Lee, G., Cowan, N., and Kirschner, M. (1988) *Science* **239,** 285–288
4. Goedert, M., Spillantini, M. G., Jakes, R., Rutherford, D., and Crowther, R. A. (1989) *Neuron* **3,** 519–526
5. Gustke, N., Trinczek, B., Biernat, J., Mandelkow, E. M., and Mandelkow, E. (1994) *Biochemistry* **33,** 9511–9522
6. Preuss, U., Biernat, J., Mandelkow, E. M., and Mandelkow, E. (1997) *J. Cell Sci.* **110,** 789–800
7. Lee, V. M. Y., Goedert, M., and Trojanowski, J. Q. (2001) *Annu. Rev. Neurosci.* **24,** 1121–1159
8. Delacourte, A., and Buee, L. (2000) *Curr. Opin. Neurol.* **13,** 371–376
9. Wischik, C. M., Novak, M., Thogersen, H. C., Edwards, P. C., Runswick, M. J., Jakes, R., Walker, J. E., Milstein, C., Roth, M., and Klug, A. (1988) *Proc. Natl. Acad. Sci. U. S. A.* **85,** 4506–4510
10. Jakes, R., Novak, M., Davison, M., and Wischik, C. M. (1991) *EMBO J.* **10,**

Downloaded from www.jbc.org at Max Planck Inst.Biophysikalische Chemie,Otto Hahn Bibl,Pf.2841,37018 Goettingen on March 23, 2009

2725–2729
11. von Bergen, M., Barghorn, S., Muller, S. A., Pickhardt, M., Biernat, J., Mandelkow, E. M., Davies, P., Aebi, U., and Mandelkow, E. (2006) *Biochemistry* **45,** 6446–6457
12. Wille, H., Drewes, G., Biernat, J., Mandelkow, E. M., and Mandelkow, E. (1992) *J. Cell Biol.* **118,** 573–584
13. von Bergen, M., Friedhoff, P., Biernat, J., Heberle, J., Mandelkow, E. M., and Mandelkow, E. (2000) *Mol. Biol. Cell* **11,** 363A–363A
14. von Bergen, M., Barghorn, S., Li, L., Marx, A., Biernat, J., Mandelkow, E. M., and Mandelkow, E. (2001) *J. Biol. Chem.* **276,** 48165–48174
15. Biernat, J., Gustke, N., Drewes, G., Mandelkow, E. M., and Mandelkow, E. (1993) *Neuron* **11,** 153–163
16. Mandelkow, E. M., Herrmann, M., and Ruhl, U. (1985) *J. Mol. Biol.* **185,** 311–327
17. Delaglio, F., Grzesiek, S., Vuister, G. W., Zhu, G., Pfeifer, J., and Bax, A. (1995) *J. Biomol. NMR* **6,** 277–293
18. Schwarzinger, S., Kroon, G. J. A., Foss, T. R., Wright, P. E., and Dyson, H. J. (2000) *J. Biomol. NMR* **18,** 43–48
19. Schwarzinger, S., Kroon, G. J. A., Foss, T. R., Chung, J., Wright, P. E., and Dyson, H. J. (2001) *J. Am. Chem. Soc.* **123,** 2970–2978
20. Johnson, B. A., and Blevins, R. A. (1994) *J. Biomol. NMR* **4,** 603–614
21. Wishart, D. S., and Sykes, B. D. (1994) *J. Biomol. NMR* **4,** 171–180
22. Wishart, D. S., and Sykes, B. D. (1994) *Methods Enzymol.* **239,** 363–392
23. Bussell, R., and Eliezer, D. (2001) *J. Biol. Chem.* **276,** 45996–46003
24. Ottiger, M., Delaglio, F., and Bax, A. (1998) *J. Magn. Reson.* **131,** 373–378
25. Farrow, N. A., Muhandiram, R., Singer, A. U., Pascal, S. M., Kay, C. M., Gish, G., Shoelson, S. E., Pawson, T., Formankay, J. D., and Kay, L. E. (1994) *Biochemistry* **33,** 5984–6003
26. Jones, J. A., Hodgkinson, P., Barker, A. L., and Hore, P. J. (1996) *J. Magn. Reson.* **113,** 25–34
27. Mukrasch, M. D., Biernat, J., von Bergen, M., Griesinger, C., Mandelkow, E., and Zweckstetter, M. (2005) *J. Biol. Chem.* **280,** 24978–24986
28. Eliezer, D., Yao, J., Dyson, H. J., and Wright, P. E. (1998) *Nat. Struct. Biol.* **5,** 148–155
29. Louhivuori, M., Paakkonen, K., Fredriksson, K., Permi, P., Lounila, J., and Annila, A. (2003) *J. Am. Chem. Soc.* **125,** 15647–15650
30. DeTure, M. A., Di Noto, L., and Purich, D. L. (2002) *J. Biol. Chem.* **277,** 34755–34759
31. Palmer, A. G., III, Kroenke, C. D., and Loria, J. P. (2001) *Methods Enzymol.* **339,** 204–238
32. Craik, D. J., and Wilce, J. A. (1997) *Methods Mol. Biol.* **60,** 195–232
33. Ackmann, M., Wiech, H., and Mandelkow, E. (2000) *J. Biol. Chem.* **275,** 30335–30343
34. Fischer, D., Mukrasch, M. D., von Bergen, M., Klos-Witkowska, A., Biernat, J., Griesinger, C., Mandelkow, E., and Zweckstetter, M. (2007) *Biochemistry* **46,** 2574–2582
35. Drewes, G., Ebneth, A., Preuss, U., Mandelkow, E. M., and Mandelkow, E. (1997) *Cell* **89,** 297–308
36. Smet, C., Leroy, A., Sillen, A., Wieruszeski, J. M., Landrieu, I., and Lippens, G. (2004) *Chembiochem.* **5,** 1639–1646
37. Eliezer, D., Barre, P., Kobaslija, M., Chan, D., Li, X. H., and Heend, L. (2005) *Biochemistry* **44,** 1026–1036
38. Tokimasa, M., Minoura, K., Hiraoka, S., Tomoo, K., Sumida, M., Taniguchi, T., and Ishida, T. (2005) *FEBS Lett.* **579,** 3481–3486
39. Barre, P., and Eliezer, D. (2006) *J. Mol. Biol.* **362,** 312–326
40. Bielska, A. A., and Zondlo, N. J. (2006) *Biochemistry* **45,** 5527–5537
41. Tjandra, N., and Bax, A. (1997) *Science* **278,** 1111–1114
42. Tolman, J. R., Flanagan, J. M., Kennedy, M. A., and Prestegard, J. H. (1995) *Proc. Natl. Acad. Sci. U. S. A.* **92,** 9279–9283
43. Bertoncini, C. W., Jung, Y. S., Fernandez, C. O., Hoyer, W., Griesinger, C., Jovin, T. M., and Zweckstetter, M. (2005) *Proc. Natl. Acad. Sci. U. S. A.* **102,** 1430–1435
44. Bernado, P., Bertoncini, C. W., Griesinger, C., Zweckstetter, M., and Blackledge, M. (2005) *J. Am. Chem. Soc.* **127,** 17968–17969
45. von Bergen, M., Barghorn, S., Biernat, J., Mandelkow, E. M., and Mandelkow, E. (2005) *Biochim. Biophys. Acta* **1739,** 158–166
46. Inouye, H., Sharma, D., Goux, W. J., and Kirschner, D. A. (2006) *Biophys. J.* **90,** 1774–1789
47. Berriman, J., Serpell, L. C., Oberg, K. A., Fink, A. L., Goedert, M., and Crowther, R. A. (2003) *Proc. Natl. Acad. Sci. U. S. A.* **100,** 9034–9038
48. Pawar, A. P., DuBay, K. F., Zurdo, J., Chiti, F., Vendruscolo, M., and Dobson, C. M. (2005) *J. Mol. Biol.* **350,** 379–392
49. Rojas Quijano, F. A., Morrow, D., Wise, B. M., Brancia, F. L., and Goux, W. J. (2006) *Biochemistry* **45,** 4638–4652
50. Goedert, M., Jakes, R., Spillantini, M. G., Hasegawa, M., Smith, M. J., and Crowther, R. A. (1996) *Nature* **383,** 550–553
51. Perez, M., Valpuesta, J. M., Medina, M., deGarcini, E. M., and Avila, J. (1996) *J. Neurochem.* **67,** 1183–1190
52. Kampers, T., Friedhoff, P., Biernat, J., and Mandelkow, E. M. (1996) *FEBS Lett.* **399,** 344–349
53. Sibille, N., Sillen, A., Leroy, A., Wieruszeski, J. M., Mulloy, B., Landrieu, I., and Lippens, G. (2006) *Biochemistry* **45,** 12560–12572
54. Barghorn, S., Davies, P., and Mandelkow, E. (2004) *Biochemistry* **43,** 1694–1703
55. Butner, K. A., and Kirschner, M. W. (1991) *J. Cell Biol.* **115,** 717–730
56. Goode, B. L., and Feinstein, S. C. (1994) *J. Cell Biol.* **124,** 769–782
57. Panda, D., Goode, B. L., Feinstein, S. C., and Wilson, L. (1995) *Biochemistry* **34,** 11117–11127
58. Goode, B. L., Denis, P. E., Panda, D., Radeke, M. J., Miller, H. P., Wilson, L., and Feinstein, S. C. (1997) *Mol. Biol. Cell* **8,** 353–365
59. Smet, C., Sambo, A. V., Wieruszeski, J. M., Leroy, A., Landrieu, I., Buee, L., and Lippens, G. (2004) *Biochemistry* **43,** 2032–2040
60. Landrieu, I., Lacosse, L., Leroy, A., Wieruszeski, J. M., Trivelli, X., Sillen, A., Sibille, N., Schwalbe, H., Saxena, K., Langer, T., and Lippens, G. (2006) *J. Am. Chem. Soc.* **128,** 3575–3583
61. Hanger, D. P., Betts, J. C., Loviny, T. L. F., Blackstock, W. P., and Anderton, B. H. (1998) *J. Neurochem.* **71,** 2465–2476
62. Morishimakawashima, M., Hasegawa, M., Takio, K., Suzuki, M., Yoshida, H., Titani, K., and Ihara, Y. (1995) *J. Biol. Chem.* **270,** 823–829

Downloaded from www.jbc.org at Max Planck Inst.Biophysikalische Chemie,Otto Hahn Bibl,Pf.2841,37018 Goettingen on March 23, 2009